FPGA Based Hardware Implementation of New Chaotic Hyperjerk System with Trigonometric Functions and, Multistability Analysis in Fractional Order Form

Rameshbabu Ramar★[1], Sundarapandian Vaidyanathan[2], Luis C. Lujano-Hernandez[3], and Jesus M. Munoz-Pacheco[4]

[1]Department of Electronics and Communication Engineering, V.S.B. Engineering College, Karur, Tamilnadu 639111 – India, Email: rrameshbabu15@gmail.com, Phone: 91 8015166025
[2]Centre for Control Systems, Vel Tech University, Vel Nagar, Chennai-600 062, India, Email: sundar@veltech.edu.in, Mobile: +91 956613754
[3]Faculty of Electronics Sciences, Benemerita Universidad Autonoma de Puebla, Av. San Claudio y 18 Sur, Puebla, 72570, Puebla, Mexico.
Email: luis.lujano@alumno.buap.mx, Mobile: +52 2214107490.
[4]Faculty of Electronics Sciences, Benemerita Universidad Autonoma de Puebla, Av. San Claudio y 18 Sur, Puebla, 72570, Puebla, Mexico.
Email: jesusm.pacheco@correo.buap.mx, Mobile: +52 2225354727

Abstract

This research article introduces a novel chaotic hyperjerk system incorporating two hyperbolic sinusoidal functions and explores its bifurcation analysis in both integer and fractional orders. The bifurcation analysis, Lyapunov spectrum analysis and phase portraits show that the proposed system exhibits wide range of complex phenomena such as chaos and multistability. The multistability phenomenon is analysed in detail with the fractional-order modelling, where the system's fractional dynamics are captured using Garappa method. The development of fractional order chaotic system results in more complex dynamical response and the presence of hyperchaos over a broad range of system parameter. Additionally, the proposed integer order hyperjerk system is implemented on a DE10-Standard digital board, which comprises a Cyclone V SE 5CSXFC6D6F31C6N FPGA to realize its chaotic behaviour for various real-time applications. The results suggest that the proposed system could serve as a promising candidate in various domains where multistability and fractional-order systems are of interest.

Keywords: Chaos, Hyperjerk, Multistability, Fractional order, FPGA Implementation

1. Introduction

Chaotic systems are very complicated dynamical systems that exhibit high sensitivity for initial conditions. The minute variations in the initial state of a chaotic system can lead to extremely different outcomes over time, providing long-term predictions nearly impossible. The understanding of chaotic systems gives a fundamental knowledge across a range of fields, including environmental engineering [1], economics [2], social sciences [3], molecular system [4], secure communication [5], Artificial intelligence [6] and optimization approach [7].

The design of chaotic hyperjerk system is an interesting topic in the field of nonlinear dynamical systems, specifically involving higher-order derivatives of position. While most traditional chaotic systems focuses on position (*x*), velocity ($\dot{x}$), acceleration ($\ddot{x}$), and jerk ($\dddot{x}$), hyperjerk systems expand this concept to the fourth time derivative, hyperjerk or snap. The design of chaotic hyperjerk systems is crucial not only for the theoretical understanding of chaos and higher order dynamics but also for practical applications that enhance the security in various industries such as cryptography [8,9], and robotics [10].

Recently, the researchers introduced many integer order chaotic hyperjerk systems with trigonometric function and analysed their complex behaviours such as coexisting attractors. For example, Leutcho et al [11] introduced a multistable chaotic hyperjerk system. Moysis [12] commenced a modified hyperjerk system with various complex features such as coexisting attractors and antimonotinicity. Vivekanandhan et al [13] presented a hyperjerk model with multiple positive Lyapunov exponents. The author discovered coexisting attractors and transient behaviours in the proposed system. Xiong et al [14] discussed extreme event and multistability behaviours in the proposed hyperjerk system. Fouodji et al [15] introduced an autonomous hyperjerk system with strange attractors. Karthikeyan et al [16] realized a snap oscillator with tan nonlinearity using electronic circuit simulation. Still exploring chaos and mutistability in hyperjerk system is indeed with fascinating challenge. The modelling of hyperjerk system using trigonometric function adds another layer of complexity due to their periodic nature. The high-dimensional systems can be designed by coupling multiple low dimensional chaotic systems [17,18] and adding more state variables [19-21]. The straightforward method to design high dimensional system is by adding more state variables with the low dimensional systems. In this work, a chaotic hyperjerk system is derived by introducing a new state variable and incorporating hyperbolic sine nonlinearities in to an existing 3D chaotic jerk system.

The hyperbolic sine nonlinearities introduce additional level of complexity which is more aggressive than simple polynomial terms.

In traditional chaotic systems, the equations of motion typically defined by integer-order derivatives. However, to solve many real-world problems such as viscoelastic models [22] and memory models [23,24], fractional order (FO) derivatives are more suitable and flexible than integer order derivatives. This brings us to the concept of FO hyperjerk (FOHJ) systems. A FOHJ system extends the idea of chaotic systems by incorporating fractional calculus, which allows the derivatives to be of non-integer order. The introduction of fractional order dynamics results in more complex dynamical response and the existence of chaos over a broad range of parameter. This enhanced chaotic behaviour has significant practical applications such as secure communication [25], image encryption [26, 27], robotics [28] and random number generation [29].

Dowei Ding et al [30] introduced a memristor based FOHJ system and discussed the extreme multistability phenomena in the proposed system. Shaohui yun et al [31] proposed a 5D FOHJ system and applied in color image encryption scheme. Fei Yu et al [32] analysed the hyperchaotic behaviour and multiscroll attractors in a FO system. Shaohui yan [33] introduced a FO chaotic system with no equilibrium points. The author also analysed the multistability and offset boosting in the proposed system. Still the exploration of chaos in fractional order chaotic hyperjerk system with hyperbolic sine nonlinearities is a challenging task.

The FPGA implementation of a chaotic hyperjerk system has significant importance since it has real time applications, The FPGA implementation is the highly valuable tool in various fields including secure communication [34, 35], and embedded systems. The primary advantages of using FPGA for implementing chaotic hyperjerk systems are parallelism, energy efficiency, high speed computation, and real word hardware computation. The key challenge is the FPGA implementation of hyperbolic sine nonlinearities in hardware, which has quite complex due to the nature these nonlinearity.

First, an integer order chaotic hyperjerk system with two hyperbolic sin nonlinearities and a cubic nonlinearity is constructed from an existing chaotic jerk system. The bifurcation and Lyapunov (LEs) plots of the proposed system are used to confirm the presence of chaotic behaviour under the various system parameters. Next, the digital hardware implementation of the new chaotic system with two hyperbolic nonlinearities is successively achieved using a Cyclone V SE 5CSXFC6D6F31C6N FPGA board. Then, a fractional order chaotic hyperjerk system is introduced and explored its dynamics using Garappa method. Finally, the multistability and coexisting attractor's behaviour is discussed using bifurcation diagram and phase portraits for the proposed fractional order system. The numerical simulation and hardware implementation indicate that the proposed system has wealthy dynamics and can be used in many practical applications.

2. Integer Order Chaotic Hyperjerk System

Recently, Ramar [36] modelled a chaotic system as given in Eq. (1).

$$\begin{aligned} \dot{p} &= q \\ \dot{q} &= r \\ \dot{r} &= ap - p^3 - b\sinh q - cr \end{aligned} \tag{1}$$

To extend to a hyperjerk system, a new state *w* is included in Eq. (1) and this corresponds to adding a fourth differential equation. The modified system is described by the differential equations as given in Eq. (2).

$$\begin{aligned} \dot{x} &= y \\ \dot{y} &= z \\ \dot{z} &= dw \\ \dot{w} &= ax - x^3 - b\sinh y - cz - \sinh z - w \end{aligned} \tag{2}$$

In the system (2) the variables are denoted as (*x*, *y*, *z*, *w)* while (*a*, *b*, *c*, *d)* represents the constants. The chaotic behaviour is observed in the system (2) when (*a*, *b*, *c*, *d)* are assigned values of (2.5,1.5,1.8,1.5). By initializing the system (2) at $X(0) = (1, 2, 1, 2)$, the Lyapunov exponents (LEs) of the system (2) are calculated over a period 1E4 seconds, resulting in $LE_1 = 0.2238$, $LE_2 = 0$, $LE_3 = -0.3972$, $LE_4 = -0.8266$. The fractal dimension (D_L) is calculated as $D_L = 2 + \frac{LE_1 + LE_2}{|LE_3|} = 2.563$, suggesting that the system (2) has chaotic attractor. The divergence of the hyperjerk system (2) can be determined as $D = \sum_{i=1}^{4} LE_i = -1$ which indicating that the system (2) has dissipative flow. Figure 1 represents the state space diagrams of the new integer-order chaotic hyperjerk system (2) with the initial condition $X(0)$.

The fixed points of the system (2) are got by solving the following equation:

$$
\begin{aligned}
&y = 0 \\
&z = 0 \\
&w = 0 \\
&ax - x^3 - b\sinh y - cz - \sinh z - w = 0
\end{aligned} \tag{3}
$$

By substituting $y = z = w = 0$ in the fourth equation of (3), we got $ax - x^3 = 0$. Since $a > 0$, there are three solutions namely, $x = 0, \pm\sqrt{a}$. Thus there are three equilibrium points given by P_0 = (0,0,0,0) and $P_{1,2} = (\pm\sqrt{a}, 0, 0, 0)$. The Jacobian matrix of the system (2) at any equilibrium points can be written as,

$$
J = \begin{bmatrix} 0 & 1 & 0 & 0 \\ 0 & 0 & 1 & 0 \\ 0 & 0 & 0 & d \\ a - 3x^2 & -b\cosh y & -c - \cosh z & -1 \end{bmatrix} \tag{4}
$$

The eigenvalues of the matrix (4) at P_0 and $P_{1,2}$ when (a,b,c,d) = (2,5, 1.5, 1.8, 1.5) are computed as (0.656, -1.205, -0.225 ± j2.166), and (-0.871 ± j1.479, 0.371 ± j1.552) respectively. This demonstrates that P_0 and $P_{1,2}$ are unstable saddle – focus fixed points.

3. Bifurcation and Lyapunov Plots

This part delves into the intricate behaviors of the new system (2) through bifurcation plot and LE spectrum across various system parameters. In general, the bifurcation plot helps to visualize the transition between the different states of the system when the parameter varies. LE spectrum are plotted to access the chaotic nature in the system, the positive LE values indicates the chaos and highly sensitivity to the initial condition nature in the system. The bifurcation plot and LE spectrum are plotted by systematically increasing any one of the parameter and keeping other parameters and initial condition fixed.

Figure 2a and Figure 2b illustrate the bifurcation diagram and set of LEs of the system (2), respectively, for a ∈ [1.7, 3]. Figure 2a shows that the system has various behaviors: a stable fixed point for $a \in [1.7 - 1.91]$, a periodic 2-cycle for $a \in [1.92 - 2.1]$, one wing chaotic attractors for $a \in [2.12 - 2.26]$ and double wing attractors for $a \in [2.27 - 3]$. Figure 2b indicates that chaotic attractors exists when $a > 2.12$. The LE spectrum show that from $a = 1.7$ to $a = 2.1$, the system has periodic motion, with $LE_1 = 0$ and LE_2, LE_3, LE_4 being negative. At the same time, when $a > 2.12$, LE_1 becomes positive, and $LE_2 = 0$, with LE_3, LE_4 remaining negative, confirming the chaotic motion in this region.

Figures (3a - 3b) depict the bifurcation diagram and set of LEs for the parameter b. It is evident from Figure 3a that the system (2) has various type of attractors when b varies between 1.3 and 2.7: chaotic attractors for $b \in [1.3, 2.1]$ with the exception of very small region, periodic attractors in the range $b \in [2.15, 2.55]$, and finally stable points. Figure 3b shows that the system has chaotic oscillation in the regions $b \in [1.3, 1.92]$ and $b \in [2, 2.1]$, where LE_1 is positive, confirming the chaotic dynamics in these intervals.

Figure 4 illustrates the bifurcation plot and LEs plot of (2) in the region from $c = 1.3$ to $c = 2.3$. Figure 4a clearly demonstrates that the system (2) has chaotic motions within the range of $c = 1.3$ and $c = 2.07$, switching to periodic motions beyond $c = 2.07$. Figure 4b reveals that $LE_1 > 0$, $LE_2 = 0$ and $LE_{3,4} < 0$ within the region $c \in [1.3, 2.07]$, confirming the chaotic nature and sensitivity on initial condition of the system in this interval.

Figure 5 depicted the bifurcation and LEs plots for the parameter d. It can be understood from Figure 5a that the system exhibits chaotic motion in the intervals $d \in [1.15, 1.7]$, with the exception of small region [1.3, 1.4] and the remaining regions are dominated by periodic motions. Figure 5b further confirms this by showing that LE_1 is positive in these regions, indicating the presence of chaos in the system.

4. FPGA Design of Integer Order Hyperjerk System

This subsection presents the FPGA based digital implementation of the proposed system (2). From the system, we realize that it is composed of nonlinearities in the form of hyperbolic trigonometric functions, i.e., sinh() in the w state variable. Therefore, a CORDIC (COordic Rotation Digital Computer) algorithm is proposed to compute the solution of the hyperjerk system. As well known, CORDIC can compute several trigonometric functions [37, 38]. On the other hand, the algorithm suffers from a reduced range $\theta \leq |1.1|$, meaning the input angle must rely on $-1.1 \leq \theta \leq +1.1$. However, the variables y and z of the hyperjerk system (2) show amplitudes closer to ±3 and ±4. As a consequence of these values, we should scale the system variables. Let us consider the following new set of variables:

$$\begin{aligned} x_1 &= fx \\ y_1 &= fy \\ z_1 &= fz \\ w_1 &= fw \end{aligned} \tag{5}$$

Where $f \in R$ represents an scaling factor. So, we obtain:

$$\dot{x}_1 = y_1$$
$$\dot{y}_1 = z_1$$
$$\dot{z}_1 = dw_1$$
$$\dot{w}_1 = ax_1 - \frac{x_1^3}{f^2} - (\frac{2b}{3})(\sinh(1.5y_1)\cosh^3(1.5y_1) + \cosh(1.5y_1)\sinh^3(1.5y_1)) - cz_1 -$$
$$(\frac{2}{3})(\sinh(1.5z_1)\cosh^3(1.5z_1) + \cosh(1.5z_1)\sinh^3(1.5z_1)) - w_1 \quad (6)$$

By proposing f = 1/6 and using the trigonometric identities:

$$\sinh(2\theta) = 2\sinh(\theta)\cosh(\theta)$$
$$\cosh(2\theta) = \cosh^2(\theta) + \sinh^2(\theta) \quad (7)$$

We obtain the scaling of the hyperjerk system:

$$\dot{x}_1 = y_1$$
$$\dot{y}_1 = z_1$$
$$\dot{z}_1 = dw_1$$
$$\dot{w}_1 = ax_1 - \frac{x_1^3}{f^2} - (\frac{2b}{3})(\sinh(1.5y_1)\cosh^3(1.5y_1) + \cosh(1.5y_1)\sinh^3(1.5y_1)) - cz_1 - \quad (8)$$
$$(\frac{2}{3})(\sinh(1.5z_1)\cosh^3(1.5z_1) + \cosh(1.5z_1)\sinh^3(1.5z_1)) - w_1$$

Figure 6 shows the state space trajectories of the modified hyperjerk system (8) obtained using the Forward Euler numerical method with integration step h = 0.01, $X(0)$ = (0.1, 0.1, 0.1, 0.1), and (a, b, c, d) = (2.5, 1.5, 1.8, 1.5). It is worth noting that by applying the previous scaling operation, the ranges for the variables are changed to $y_1 \leq |1.5\ (\pm 0.4)|$ and $z_1 \leq |1.5\ (\pm 0.6)|$, respectively, and can now be handled by the CORDIC algorithm.

The next step consists of determining the fixed-point digital representation. Since the maximum and minimum values for the system solution are $1/f = 6$ and $z_1 = -0.6$, respectively, we choose a digital format Q3, 28, i.e., three bits allocated for the whole value part and the remaining bits for the decimal part. Figure 7 describes the main blocks of the digital design, where *Euler* block calculates the solution in every clock-rising transition. The hyperjerk system was implemented on a DE10-Standard digital board comprising a Cyclone V SE 5CSXFC6D6F31C6N FPGA. Also, a 12-bit high-speed data converter DAC312 is used for data visualization on an oscilloscope.

On the other hand, Figure. 8 shows the RTL schematic which consists of the following parts:

(a) To synchronize the operation frequency of the numerical algorithm in block *Hyperjerk:S2*, the input *clk 50MHZ* enables a 50 MHz clock, which is then divided by a frequency divisor of 50 KHz (20 us) clock for Euler Block (*HyperJerk TIMER:S0*) and 5 MHz (200 ns) clock for CORDIC Hyperbolic blocks (*CORDIC Timer:S1*).

(b) In addition, the block *Hyperjerk:S2* computes system variables x_1, y_2, z_3, w_4 of hyperjerk system, which are labeled as $x[31:0]$, $y[31:0]$, $z[31:0]$, and $w[31:0]$, respectively.

(c) To obtain phase portraits of chaotic attractors, it is possible to select pairs of variables for conversion via the DAC device (*DAC Block:S3,S4*).

Listing 1 shows the pseudocode for the Hyperjerk block (*S2*) in Figure 8.

```
MODULE Hyperjerk (x,y,z,w,clk_CORDIC,clk_Hyperjerk,rst);
      OUTPUT: x,y,z,w;
      INPUT : clk_CORDIC,clk_Hyperjerk,rst;
      REGISTER SIGNED: xt0,yt0,zt0,wt0;
GENERATE
      Euler
x_t0(xt0),.y_t0(yt0),.z_t0(zt0),.w_t0(wt0),.x(tp1),.y(tp2),.z(
tp3),.
      w(tp4),clk_CORDIC,clk_Hyperjerk;
ENDGENERATE
ALWAYS @(POSEDGE clk_Hyperjerk) BEGIN
      IF (rst == 1) BEGIN
            xt0 = 'h01999999;
            yt0 = 'h01999999;
            zt0 = 'h01999999;
            wt0 = 'h01999999;
      END
      ELSE BEGIN
            xt0 = tp1;
            yt0 = tp2;
            zt0 = tp3;
            wt0 = tp4;
      END
ENDALWAYS
ASSIGN  tp1  TO  x;
ASSIGN  tp2  TO  y;
ASSIGN  tp3  TO  z;
ASSIGN  tp4  TO  w;
ENDMODULE
```

Listing 1: Verilog synthesis of the Hyperjerk module (S2) of Figure 8 for FPGA implementation

To find a solution for the new hyperjerk system, we employ the Forward-Euler algorithm described in the Verilog hardware description language (Listing 2). For the Euler module, we use an integration step of h = 0.01, while the product of state variables requires a 32-bit multiplier module.

```
MODULE Euler (x_t0, y_t0, z_t0, w_t0, x, y, z, w, clk_Euler,clk_CORDIC);
    PARAMETERS: h = 0.01, a= 2.5, b= 1.5, c= 1.8, d= 1.5 // Fixed-Point
    OUTPUTS: x, y, z, w;
    INPUTS: x_t0, y_t0, z_t0, w_t0, clk_Euler,clk_CORDIC;
    WIRES SIGNED: r_x, r_y, r_z, r_w;
    GENERATE
        MULTIPLY: phase_1_5_y = (1.5)(y_t0);
        MULTIPLY: phase_1_5_y = (1.5)(z_t0);
        CORIDIC_H: (phase_1_5_y,cosh_CORDIC_out_y, sinh_CORDIC_out_y,clk_CORDIC);
        CORIDIC_H: (phase_1_5_y,cosh_CORDIC_out_y, sinh_CORDIC_out_y,clk_CORDIC, flag_CORDIC);
        //-----------------
        MULTIPLY: temp1 = (h)(y_t0);
        ASSIGN r_x = temp1 + x_t0;   //x
        //-----------------
        MULTIPLY: temp2 = (h)(z_t0);
        ASSIGN r_y = temp2 + y_t0;   //y
        //-----------------
        MULTIPLY: temp3 = (d)(w_t0);
        MULTIPLY: temp4 = (h)(temp3);
        ASSIGN r_z = temp4 + z_t0;   //z
        //-----------------
        MULTIPLY temp5 = (a)(x_t0);
       MULTIPLY temp6 = (x_t0)(x_t0);
       MULTIPLY temp7 = (temp6)(x_t0);
       MULTIPLY temp8 = (temp7)(f_x_inv);
       MULTIPLY temp9 = (temp8)(f_x_inv);
       MULTIPLY temp10 = (sinh_CORDIC_out_y)(cosh_CORDIC_out_y);
       MULTIPLY temp11 = (temp10)(cosh_CORDIC_out_y);
       MULTIPLY temp12 = (temp11)(cosh_CORDIC_out_y);
       MULTIPLY temp13 = (temp10)(sinh_CORDIC_out_y);
       MULTIPLY temp14 = (temp13)(sinh_CORDIC_out_y);
       ASSIGN   temp15 = temp12 + temp14;
       MULTIPLY temp16 = (c)(z_t0);
       MULTIPLY temp17 = (sinh_CORDIC_out_z)(cosh_CORDIC_out_z);
       MULTIPLY temp18 = (temp17)(cosh_CORDIC_out_z);
       MULTIPLY temp19 = (temp18)(cosh_CORDIC_out_z);
       MULTIPLY temp20 = (temp17)(sinh_CORDIC_out_z);
       MULTIPLY temp21 = (temp20)(sinh_CORDIC_out_z);
       ASSIGN   temp22 = temp19 + temp21;
```

```
        MULTIPLY temp23 = (temp22)(f_w_4);
        ASSIGN    temp24 = temp5 - temp9 - temp15 - temp16 -
temp23 - w_t0;
        MULTIPLY temp25 = (h)(temp24);
        ASSIGN r_w = temp25 + w_t0;    //w
    ENDGENERATE
    always @(posedge flag_CORDIC)begin
            ASSIGN: x = r_x;
        ASSIGN: y = r_y;
        ASSIGN: z = r_z;
        ASSIGN: w = r_w;
    end
ENDMODULE
```

Listing 2: Verilog synthesis for digital design of the proposed Hyperjerk in the FPGA

After that, the resulting digital outputs are converted to analog ones by DAC312 only for visualization purposes. Since DAC312 requires a 250ns stabilization time, eight clock cycles are chosen to obtain 20us with a master clock of 50MHz by using the module *HyperJerk TIMER*. Finally, the DAC output block (S3,S4) in Figure. 8 is custom-designed for each output signal *x*, *y*, *z*, *w*. Figure 9 depicts the experimental setup of the new HyperJerk system implemented on a DE10-Standard digital board, which comprises a Cyclone V SE 5CSXFC6D6F31C6N FPGA. The hardware resources utilization is summarized in Table 1.

We have found that the main limitation associated with implementing the hyper jerk system in FPGAs can be the scaling factor required to change the maximum and minimum values of the chaotic signals, as shown in Eq. (5) to Eq. (8). For instance, in the case of high-dimensional systems comprising more than three state variables, the change of variable becomes cumbersome and yields more intricate expressions, which may result in more FPGA resource utilization and power consumption. In particular, the challenge for the chaotic hyperjerk system arises from implementing the CORDIC architecture as the algorithm is constrained within the interval $\pm\pi/2$ to generate the sinh(.) function.

Regarding performance benchmarking, we perform the following studies. The power analysis was conducted using the Power Analyzer Tool provided by Quartus design software, which considers a toggle rate for the input/output signals while the remaining signals are fixed at 12.5%. Furthermore, the Timing Analysis considers a Master Clock with a period of 20 ns (50 MHz), a rise time of 0 ns, and a fall time of

10 ns for the input pin indicated as clk_50MHZ. The obtained results and comparison with other FPGA implementations of chaotic systems are given in Table 2. For example, the study conducted in [39] focuses on a double displacement system with three variables and demonstrates superior performance in terms of static power; however, the dynamic and I/O power consumption is predominantly higher than that of the proposed design. The works in [40] and [41] relate to chaotic systems with four and three variables, respectively, and do not report power consumption. Nonetheless, it can be noticeable that these two systems operate at a maximum frequency lower than the proposed architecture herein, indicating a higher processing speed performance with a high bit throughput of 5.8 Gbps.

Associated with the power consumption analysis in Table 2, the cooling requirements demand a 23 mm heat sink with an airflow rate of 200 LFpM, resulting in a total thermal power dissipation of 444.67 mW. Using the Quartus design software, the FPGA results in this work are obtained by establishing an operation scenario with a temperature of about 85°C, indicating 3.4 times the ambient temperature. This setting ensures optimal functionality in environments categorized as hot. However, it is important to note that the chaotic attractor results were acquired in a controlled laboratory environment, eliminating the potential effects of noise that could interfere with real-time data acquisition. The proposed FPGA design for the hyperjerk system has one input and two outputs. So, with the help of the Signal Tap Logic Analyzer in Quartus, we have not identified any abnormal operation of the chaotic outcomes. Since the signal tap logic analyzer operates in real time, the output data cannot be stored. Therefore, presenting empirical evidence of proper functionality is crucial, as illustrated in Figure 10.

Finally, the outcomes of the FPGA implementation of the new chaotic hyperjerk system are shown in Figure 10, which are contrasted with the ones delivered by Matlab. More particularly, we plot the phase planes *xy*, *yz*, *zw*, and *xw*, respectively. We found a strong correlation between numerical results and FPGA implementation, validating the chaos generation of the new proposed system.

5. Fractional – Order Chaotic Hyperjerk (FOHJ) System

A FOHJ system is a system where the governing equations are based on fractional-order derivatives of the state variables. The fractional-order systems typically take the form:

$$\begin{aligned} D_t^q x &= y \\ D_t^q y &= z \\ D_t^q z &= w \\ D_t^q w &= f(x,y,z,w) \end{aligned} \tag{9}$$

Here, D^q represents the fractional derivative of order q (with $0 < q < 1$), x, y, z, and w represent states of the system, $f(x,y,z,w)$ is a nonlinear function that governs the chaotic behavior of the system. Let us define a new FOHJ system as follows:

$$\begin{aligned} D_t^q x &= y \\ D_t^q y &= z \\ D_t^q z &= dw \\ D_t^q w &= ax - x^3 - b\sinh y - cz - \sinh z - w \end{aligned} \tag{10}$$

In the FOHJ system (10), $q = 0.99$, and $a = 6.5$, $b = d = 1.5$, $c = 1.8$. The LEs of the FOHJ system (10), computed with a simulation time of 10,000 and an initial condition of (1,1,1,1), are (LE_1, LE_2, LE_3, LE_4) = (0.2682, 0, −0.4602, −0.9314), demonstrating its chaotic nature. The Lyapunov dimension of FOHJ system (10), given by $D_L = 2 + [(L_1 + L_2)/|L_3|] = 2.2879$ which is fractal.

To solve fractional order differential equations many numerical methods such as Garappa method [42], Grünwald–Letnikov method [43], Laplace transform [44] and spectral methods [45] are available. In this work, we selected the Garappa method to solve the proposed FOCHJ system due its accuracy and efficiency. It offers a reliable numerical stability, making it well-suited for simulating complex fractional-order chaotic systems. While other methods may offer similar accuracy, they are complex to implement and also require more computation time.

The proposed FOHJ system (10) is simulated by using Roberto Garrappa method employing the step size of 0.005. Figure 11 shows the phase portraits of the new FOHJ system with the initial condition (1,1,1,1).

The bifurcation and LEs plot for FOHJ system (10) under the fractional order q are depicted in Figure 12. Figure 12a specify that the FOHJ system (10) has chaotic motion in the region ranges from $q = 0.97$ to $q = 1$. Figure 12b illustrates the LEs plot as the fractional order q varies within the range [0.95,1], revealing that the system has chaotic behavior specifically for $q \in [0.97, 1]$.

6. Multistability in Fractional Order Hyperjerk System

Multistability and coexisting phenomenon is a special feature of chaotic system by which the system can able to produce multiple coexisting attractors under the same set of system parameters. In this section, we explored the multistability and coexisting phenomenon in the proposed fractional order hyperjerk system (10).

Recently, Liu [46] analyzed multistability in the fractional order multiwing chaotic system, Ren et al [47] discovered extreme multistability in their proposed system. In secure communication system, multistability and coexisting attractors enhances the security of the system since it make very difficult to predict the system behavior. The multiple attractors can be used to represent different symbols in the information encoding [48, 49]. To enhance stability, the adaptive control techniques such as fractional order sliding mode controllers [50], backstepping controllers [51] can be integrated to maintain the desired dynamics. Additionally, various synchronization methods [52, 53] ensure the recovery of reliable signal under varying initial conditions.

Figure 13a illustrates the bifurcation behavior of the FOHJ system (10) for specific value of a, displaying the results of two different initial conditions: One set of conditions (0.1,0.1,0.1,0.1) in blue and another set (0.1,-0.1,-0.1,-0.1) in red. The clear separation between the blue and red branches within the range $a \in [1, 5]$ signifies the occurrence of multiple stable states, including periodic oscillation and chaotic attractors, with in the system (10). This bifurcation pattern highlights the system's complex dynamics over this parameter range. The overlapping of the blue and red branches in the region $a \in [5.5, 8]$ suggests the existence of a single chaotic attractor within that parameter range. Figure 13b supports that the system (10) has chaotic attractors where LE_1 (Blue) has positive values.

Further, to validate the multistability in the FOHJ system (10), the bifurcation for c with the set of initial conditions (0.1,0.1,0.1,0.1) (blue) and (0.1,-0.1,-0.1,-0.1) (red) are plotted as give in Figure 15a. The non-overlapping of the blue and red branches in the range $c \in [3, 5]$ indicates the occurrence of coexisting attractors in periodic and chaotic regions in the system (10). As depicted in Figure 15b, the system (10) exhibits intricate chaotic dynamics within the region $c \in [1, 3.5]$ where LE_1 in Blue takes on positive values. This suggests the presence of strong dependence on initial positions, a key characteristic of chaotic behavior in the system. The various coexisting attractors in various c values are shown in Figure 16.

Conclusion

This study proposes a new chaotic hyperjerk system with two hyperbolic functions, along with a detailed dynamical analysis that highlight its wealthy chaotic behavior, including Lyapunov exponents, and bifurcations. The dynamic characteristics of the proposed system were thoroughly examined using numerical simulations and theoretical study. Furthermore, we successfully implemented the proposed integer order chaotic hyperjerk system on an FPGA platform, demonstrating its feasibility and efficient hardware realization. Further, we introduced a fractional order hyperjerk system, which is designed from the proposed integer order system. Through an in-depth multistability analysis, we observed the initial conditions based coexistence of multiple attractors within the system. The results show that fractional-order dynamics can significantly enhance the usability of chaotic systems in areas like secure communication and nonlinear control.

References

1. Chakraborty, A. and Veeresha, P. "Effects of global warming, time delay and chaos control on the dynamics of a chaotic atmospheric propagation model within the frame of Caputo fractional operator", *Communications in Nonlinear Science and Numerical Simulation*, **128**, Article ID 107657, 2024. https://doi.org/10.1016/j.cnsns.2023.107657.

2. Koca, I. "Financial model with chaotic analysis", *Results in Physics*, **51**, Article ID 106633, 2024. https://doi.org/10.1016/j.rinp.2023.106633.

3. Boubaker, O. "Chaos in Physiological Control Systems: Health or Disease?", *Chaos Theory and Applications*, **6(1),** pp.1-12, 2023. https://doi.org/10.51537/chaos.1413955.

4. Qin, W., Li, H., Jiang, Z. et al. "Generation and analysis of the chaos phenomenon in the molecular-distillation-Navier–Stokes (MDNS) nonlinear system", *Frontiers in Physics*, **12**, Article ID 1400973, 2024. https://doi.org/10.3389/fphy.2024.1400973.

5. Li, M.J., Zhou, X.F., Wang, F., et al. "Research on chaotic secure optical communication system based on dispersion keying with time delay signatures concealment", *Chaos, Solitons & Fractals*, **182**, Article ID 114720, 2024. https://doi.org/10.1016/j.chaos.2024.114720.

6. Jia, B., Wu, H. and Guo, K., "Chaos theory meets deep learning: A new approach to time series forecasting", *Expert Systems with Applications*, **255**, Article ID.124533, 2024. https://doi.org/10.1016/j.eswa.2024.124533.
7. Xu, L., Ma, R.R., Wu, J. and Rao, P., "Proximal policy optimization approach to stabilize the chaotic food web system", *Chaos, Solitons & Fractals*, **192,** Article ID.116033, 2025. https://doi.org/10.1016/j.chaos.2025.116033.
8. Yu, J., Xie, W., Zhong, Z. and Wang, H., "Image encryption algorithm based on hyperchaotic system and a new DNA sequence operation", Chaos, Solitons & Fractals, **162**, Article ID.112456, 2022. https://doi.org/10.1016/j.chaos.2022.112456
9. Sambas, A., Miroslav, M., Vaidyanathan, S., et al., "A new hyperjerk system with a half line equilibrium: Multistability, period doubling reversals, antimonotonocity, electronic circuit, FPGA design, and an application to image encryption", IEEE Access, **12**, pp.9177-9194, 2024. https://doi.org/10.1109/ACCESS.2024.3351693
10. Ban, C., Cai, G., Wei, W. et al., "Dynamic response and chaotic behavior of a controllable flexible robot", *Nonlinear Dynamics*, **109(2),** pp.547-562, 2022. https://doi.org/10.1007/s11071-022-07405-7
11. Leutcho, G.D., Kengne, J. and Kengne, L.K., "Dynamical analysis of a novel autonomous 4-D hyperjerk circuit with hyperbolic sine nonlinearity: chaos, antimonotonicity and a plethora of coexisting attractors", *Chaos, Solitons & Fractals*, **107**, pp.67-87, 2028. https://doi.org/10.1016/j.chaos.2017.12.008.
12. Moysis, L., Petavratzis, E., Marwan, M. et al., "Analysis, synchronization, and robotic application of a modified hyperjerk chaotic system", *Complexity*, **2020(1),** p.2826850, 2020. https://doi.org/10.1155/2020/2826850
13. Vivekanandhan, G., Chedjou, J.C., Jacques, K. et al., "A unique self-driven 5D hyperjerk circuit with hyperbolic sine function: Hyperchaos with three positive exponents, complex transient behavior and coexisting attractors", *Chaos, Solitons & Fractals*, **186**, Article ID.115276, 2024. https://doi.org/10.1016/j.chaos.2024.115276.
14. Xiong, Y., Zhang, X., Chedjou, J.C. et al., "Super extreme event and coexisting attractors in a novel chaotic snap system with hyperbolic sine function: Theoretical investigations and circuit experiments", *Chaos, Solitons & Fractals*, **193**, p.116061. 2025. https://doi.org/10.1016/j.chaos.2025.116061.
15. Fouodji Tsotsop, M., Kengne, J., Kenne, G. et al., "Coexistence of multiple points, limit cycles, and strange attractors in a simple autonomous hyperjerk circuit with hyperbolic sine function", *Complexity*, **2020(1),** Article ID.6182183, 2020. https://doi.org/10.1155/2020/6182183.

16. Rajagopal, K., Jafari, S., Akgul, A. et al., "A simple snap oscillator with coexisting attractors, its time-delayed form, physical realization, and communication designs", *Zeitschrift für Naturforschung A*, **73(5),** pp.385-398, 2018. https://doi.org/10.1515/zna-2017-0426

17. Abdulaali, R.S., Jamal, R.K. and Mousa, S.K., "Generating a new chaotic system using two chaotic Rossler-Chua coupling systems", *Optical and Quantum Electronics*, **53**, pp.1-10. 2021, https://doi.org/10.1007/s11082-021-03341-9

18. Rech, P.C., "Complex Dynamics of a Linear Coupling of Two Chaotic Lorenz Systems", *Brazilian Journal of Physics*, **54(1),** Article ID.15. 2024. https://doi.org/10.1007/s13538-023-01392-9

19. Tiwari, A., Singh, P.P. and Roy, B.K., "A realizable chaotic system with interesting sets of equilibria, characteristics, and its underactuated predefined-time sliding mode control", *Chaos, Solitons & Fractals*, **185**, Article ID.115179, 2024. https://doi.org/10.1016/j.chaos.2024.115179

20. Yan, S., Wang, J., Wang, E., et al. "A four-dimensional chaotic system with coexisting attractors and its backstepping control and synchronization", *Integration*, **91**, pp.67-78, 2023. https://doi.org/10.1016/j.vlsi.2023.03.001

21. Fu, S., Cheng, X. and Liu, J. "Dynamics, circuit design, feedback control of a new hyperchaotic system and its application in audio encryption". *Scientific Reports*, **13(1),** Article ID.19385, 2023. https://doi.org/10.1038/s41598-023-46161-5

22. Gao, Y., Yin, D., Tang, M. et al., "A three-dimensional fractional visco-hyperelastic model for soft materials", *Journal of the Mechanical Behavior of Biomedical Materials*, **137,** Article ID .105564, 2023. https://doi.org/10.1016/j.jmbbm.2022.105564

23. He, S., Wang, H. and Sun, K. "Solutions and memory effect of fractional-order chaotic system: A review", *Chinese Physics B*, **31(6),** p.060501, 2023. https://doi.org/10.1088/1674-1056/ac43ae

24. Dutta, M. and Roy, B.K., "A new memductance-based fractional-order chaotic system and its fixed-time synchronization", *Chaos, Solitons & Fractals*, **145**, Article ID.110782, 2021. https://doi.org/10.1016/j.chaos.2021.110782

25. Iqbal, S. and Wang, J., "A novel fractional-order 3-D chaotic system and its application to secure communication based on chaos synchronization", *Physica Scripta*, **100(2),** Article ID.025243, 2025. https://doi.org/10.1088/1402-4896/ad9cfe

26. Ghasemi, G., Parvaz, R. and Khedmati Yengejeh, Y., “Three-Dimensional and Multiple Image Encryption Algorithm Using a Fractional-Order Chaotic System”, *Computation*, **13(5),** Article ID.115, 2025. https://doi.org/10.3390/computation13050115

27. Akgül, A., Yaz, M. and Emin, B., “Chaos-based approaches to digital data security: Analysis of incommensurate fractional-order Arneodo chaotic system and engineering application on Nvidia Jetson AGX Orin”, *Integration*, Article ID.102355, 2025. https://doi.org/10.1016/j.vlsi.2025.102355

28. Cui, Y. and Zheng, Z., “Novel Fractional-Order Chaotic System Applied to Mobile Robot Path Planning and Chaotic Path Synchronization”, Symmetry**, 17(3),** Article ID.350, 2025. https://doi.org/10.3390/sym17030350

29. Akmeşe, Ö.F., “A novel random number generator and its application in sound encryption based on a fractional-order chaotic system”, *Journal of Circuits, Systems and Computers*, **32(03),** p.2350127, 2023. https://doi.org/10.1142/S021812662350127X

30. Ding, D., Xu, X., Yang, Z et al., “Extreme multistability of fractional-order hyperchaotic system based on dual memristors and its implementation”, *Chaos, Solitons & Fractals*, **183**, Article ID.114878, 2023. https://doi.org/10.1016/j.chaos.2024.114878

31. Yan, S., Jiang, D., Cui, Y. et al., “A fractional-order hyperchaotic system that is period in integer-order case and its application in a novel high-quality color image encryption algorithm”, *Chaos, Solitons & Fractals*, **182,** Article ID.114793, 2024. https://doi.org/10.1016/j.chaos.2024.114793

32. Yu, F., Xu, S., Lin, Y. et al., “Design and analysis of a novel fractional-order system with hidden dynamics, hyperchaotic behavior and multi-scroll attractors”, *Mathematics*, **12(14),** Article ID.2227, 2024. https://doi.org/10.3390/math12142227

33. Yan, S., Wang, E. and Wang, Q., “Analysis and circuit implementation of a non-equilibrium fractional-order chaotic system with hidden multistability and special offset-boosting”, *Chaos: An Interdisciplinary Journal of Nonlinear Science*, **33(3).**2023. https://doi.org/10.1063/5.0130083

34. Luo, Y., Fan, C., Xu, C. et al., “Design and FPGA implementation of a high-speed PRNG based on an nD non-degenerate chaotic system”, *Chaos, Solitons & Fractals*, **183**, Article ID.114951, 2023. https://doi.org/10.1016/j.chaos.2024.114951

35. Zhang, J., Wang, P., Cheng, N. et al., "The dynamic analysis, FPGA implementation, and adaptive synchronization control application of a multi-vortex chaotic system based on nonlinear functions", *The Journal of Supercomputing*, **80(16),** pp.24379-24412, 2024. https://doi.org/10.1007/s11227-024-06257-9

36. Ramar, R., Vaidyanathan, S., Akgul, A. et al., "A new chaotic jerk system with cubic and hyperbolic sine nonlinearities and its application to random number generation and biomedical image encryption", Article in Press, *Scientia Iranica*, 2024. DOI: 10.24200/sci.2024.63254.8303

37. Fu, W., Xia, J., Lin, X. et al. "Low-latency hardware implementation of high-precision hyperbolic functions sinh x and cosh x based on improved cordic algorithm", *Electronics*, **10(20),** p.2533, 2021. https://www.mdpi.com/2079-9292/10/20/2533.

38. Ardavan Vakil and Miad Faezipour. "Toward CORDIC-based Hyperbolic Function Implementation for Neural Engineering Hardware". In: 2022 International Conference on Computational Science and Computational Intelligence (CSCI). pp. 416–418, 2022. doi: 10.1109/CSCI58124.2022.00080

39. Gugapriya, G., Duraisamy, P., Karthikeyan A. et al., "Fractional-order chaotic system with hyperbolic function", *Advances in Mechanical Engineering*, **11(8),** 2029. https://doi.org/10.1177/1687814019872

40. Karakaya, B., Gülten, A., Frasca M. "A true random bit generator based on a memristive chaotic circuit: analysis, design and FPGA implementation", *Chaos, Solitons & Fractals*, **119**, pp. 143–9, 2019. https://doi.org/10.1016/j.chaos.2018.12.021

41. Mohammad S. "Chaotic dynamics of discrete memristor-coupled Sinh map", *Chaos, Solitons & Fractals*, **196,** Article ID. 116480, 2025. https://doi.org/10.1016/j.chaos.2025.116480

42. Garrappa, R., "Numerical solution of fractional differential equations: A survey and a software tutorial", *Mathematics*, **6(2),** Article ID.16, 2018. https://doi.org/10.3390/math6020016

43. Scherer, R., Kalla, S.L., Tang, Y. et al., "The Grünwald–Letnikov method for fractional differential equations", Computers & Mathematics with Applications, **62(3),** pp.902-917, 2011. https://doi.org/10.1016/j.camwa.2011.03.054

44. Soradi-Zeid, S., Mesrizadeh, M. and Cattani, C., "Numerical solutions of fractional differential equations by using Laplace transformation method and quadrature rule", *Fractal and Fractional*, **5(3),** Article ID.111, 2021. https://doi.org/10.3390/fractalfract5030111

45. Papadopoulos, I.P. and Olver, S., “A sparse spectral method for fractional differential equations in one-spatial dimension”, *Advances in Computational Mathematics*, **50(4),** Article ID.69, 2024. https://doi.org/10.1007/s10444-024-10164-1

46. Liu, T., Sun, B., Li, P. et al., “Multistability Analysis of a Fractional-Order Multi-Wing Chaotic System and its Circuit Realization”, *Mobile Networks and Applications*, **29(3),** pp.603-613, 2024. https://doi.org/10.1007/s11036-023-02155-1

47. Ren, L., Li, S., Banerjee, S. et al., “A new fractional-order complex chaotic system with extreme multistability and its implementation”, *Physica Scripta*, **98(5),** Article ID.055201, 2023. https://doi.org/10.1088/1402-4896/acc6a3

48. Qin, M. and Lai, Q., “Multistability, amplitude control and image encryption in a novel chaotic system with one equilibrium”, *Indian Journal of Physics*, **98(2),** pp.701-715, 2024. https://doi.org/10.1007/s12648-023-02815-8

49. Xin, Z.J. and Lai, Q., “Dynamical investigation and encryption application of a new multiscroll memristive chaotic system with rich offset boosting features”, *Chaos, Solitons & Fractals*, **181**, Article ID.114696, 2024. https://doi.org/10.1016/j.chaos.2024.114696

50. Zhang, M., Zang, H. and Liu, Z., “Fractional-order adaptive sliding mode control based on predefined-time stability for chaos synchronization”, *Chaos, Solitons & Fractals*, **191**, Article ID.115921, 2025. https://doi.org/10.1016/j.chaos.2024.115921

51. Bai, Z., Li, S., Liu, H. et al., “Adaptive fuzzy backstepping control of fractional-order chaotic system synchronization using event-triggered mechanism and disturbance observer”, *Fractal and Fractional*, **6(12),** Article ID.714, 2022. https://doi.org/10.3390/fractalfract6120714

52. You, J. and Zhang, Z., “Finite-time synchronization of fractional order chaotic systems by applying the maximum-valued method of functions of five variables”, *AIMS Math*, **10(3),** pp.7238-7255, 2025. doi: 10.3934/math.2025331

53. Nabil, H. and Tayeb, H., “Modified generalized projective synchronization of the geomagnetic Krause and Robert fractional-order chaotic system and its application in secure communication”, *The European Physical Journal B*, **98(4),** Article ID.56, 2025. https://doi.org/10.1140/epjb/s10051-025-00897-3

Biographies of Authors

Rameshbabu Ramar received the Ph.D degree in Electronics and Communication Engineering from St.Peter University at Chennai, Tamilnadu, India in 2021. He is currently a Associate Professor at the Department of Electronics and Communication Engineering, V.S.B Engineering College, Karur, Tamilnadu, India. He has published many Scopus-indexed research publications in international journals. His current research interests include design of chaotic and hyperchaotic systems, FPGA implementation, Adaptive control, and Chaos Synchronization.

Sundarapandian Vaidyanathan received the D.Sc. degree in Electrical and Systems Engineering from Washington University at St. Louis, St. Louis, MO, USA, in 1996. He is currently a Professor at the Research and Development Centre, Vel Tech University, Chennai, India. He has published over 600 Scopus-indexed research publications in international journals. His current research interests include linear and nonlinear control systems, chaotic and hyperchaotic systems, circuits, data science, mathematical modelling, and scientific computing.

Luis C. Lujano-Hernandez received the B.S. degree in Electronic Engineering in 2019. He received the M.S. degree in Electronic Engineering from the Faculty of Electronics Sciences (FCE) of the Benemerita Universidad Autonoma de Puebla (BUAP) in 2021, where he is currently pursuing his PhD in Applied Research in Industry. His research interests include analog design, FPGA design, chaotic systems, fractional-order calculus, and, more recently, chaotic neural networks.

Jesus M. MunozPacheco obtained his PhD in Electronic Sciences from INAOE in 2009. In 2012, he joined BUAP as a Full Professor-Researcher. He is also the Academic Coordinator of the Doctoral Program in Electronics and Head of the Chaos, Fractals, and Complexity research group. Dr. Munoz-Pacheco has been included in the "Stanford-Elsevier" World’s Top 2% Scientists List (for both single-year and career performances) for the sixth consecutive year, 2020-2025. He is also ranked in the Top 0.5% of all scholars worldwide (No. 72 in Chaos theory) according to the most recent 2024 ScholarGPS. His research interests are dynamical systems, chaotic oscillators, circuits, and fractional calculus. He is currently an associate editor for several indexed journals.

List of Figures:

List of Tables:

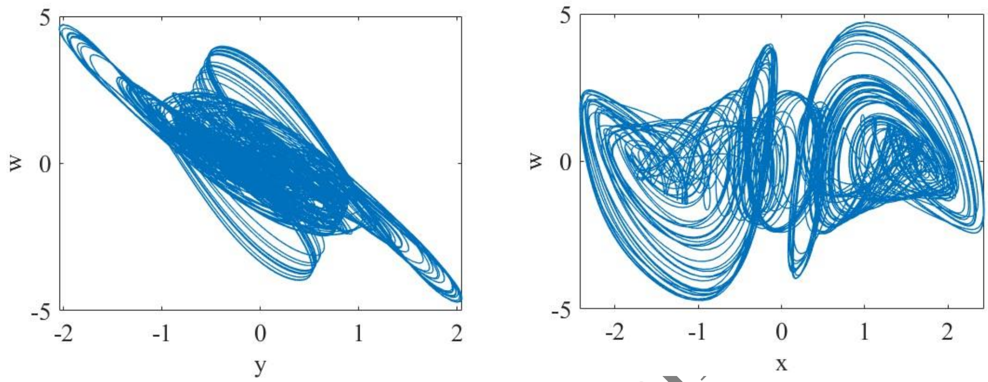

(a) (b)

Figure 1 : The state space trajectories of the new chaotic hyperjerk system (2)

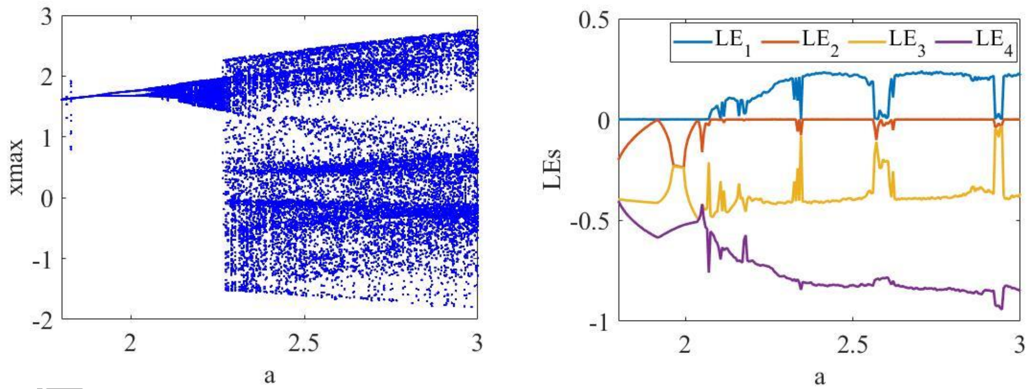

(a) (b)

Figure 2: (a) Bifurcation (b) LEs plots for the parameter *a*

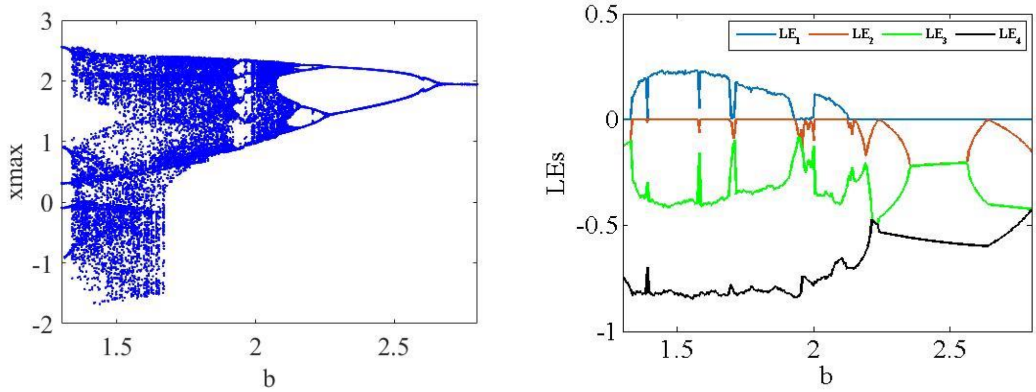

(a) (b)

Figure 3: (a) Bifurcation (b) LEs plots for the parameter *b*

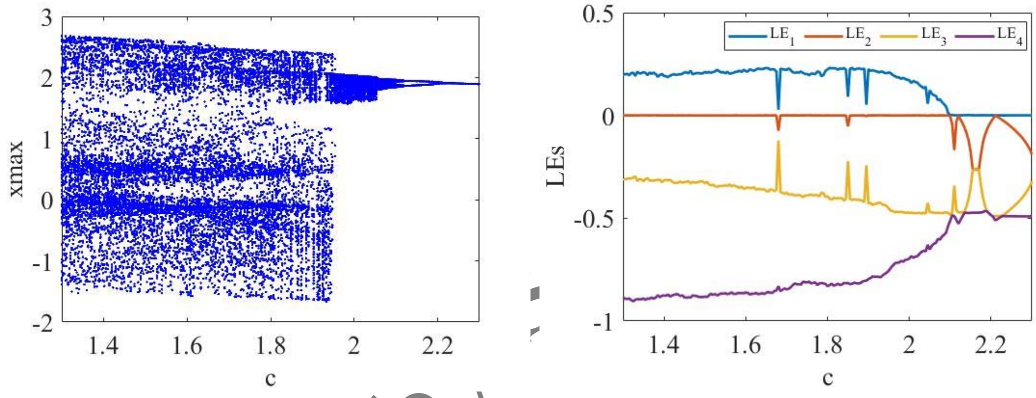

(a) (b)

Figure 4: (a) Bifurcation plot and (b) LEs plot for the parameter *c*

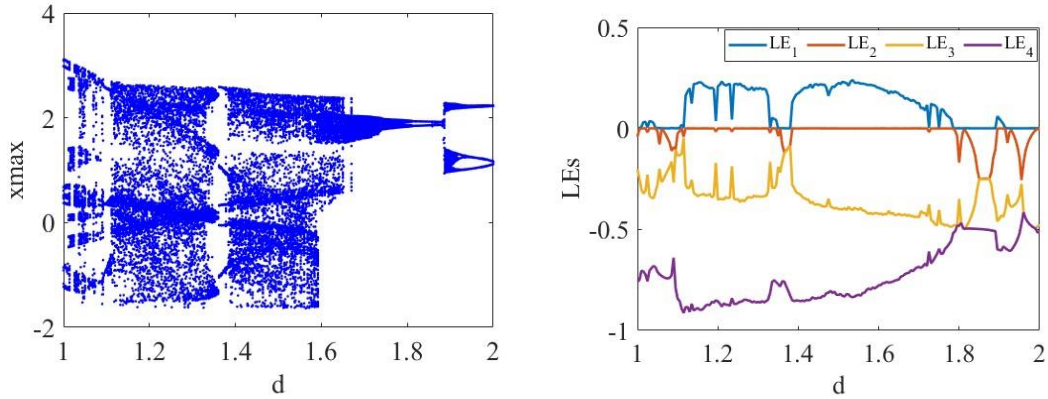

(a) (b)

Figure 5: (a) Bifurcation (b) LEs plots for the parameter *d*

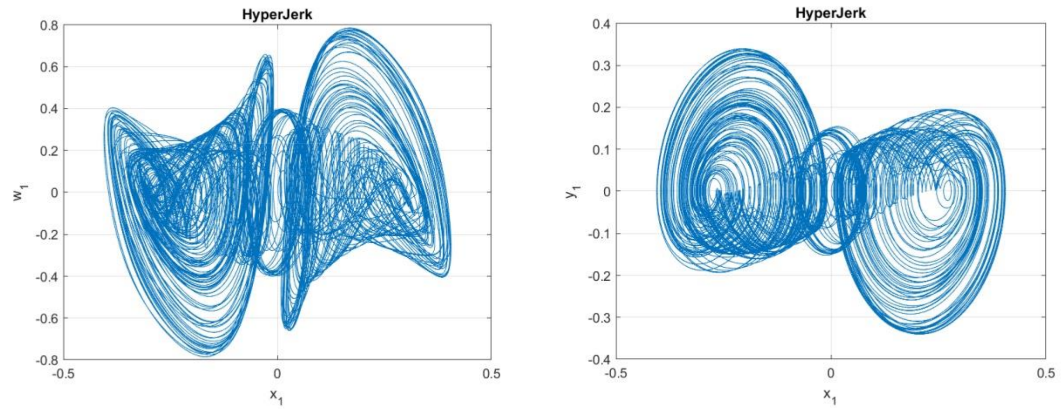

Figure 6: The attractors of the chaotic hyperjerk system under a scaling procedure.

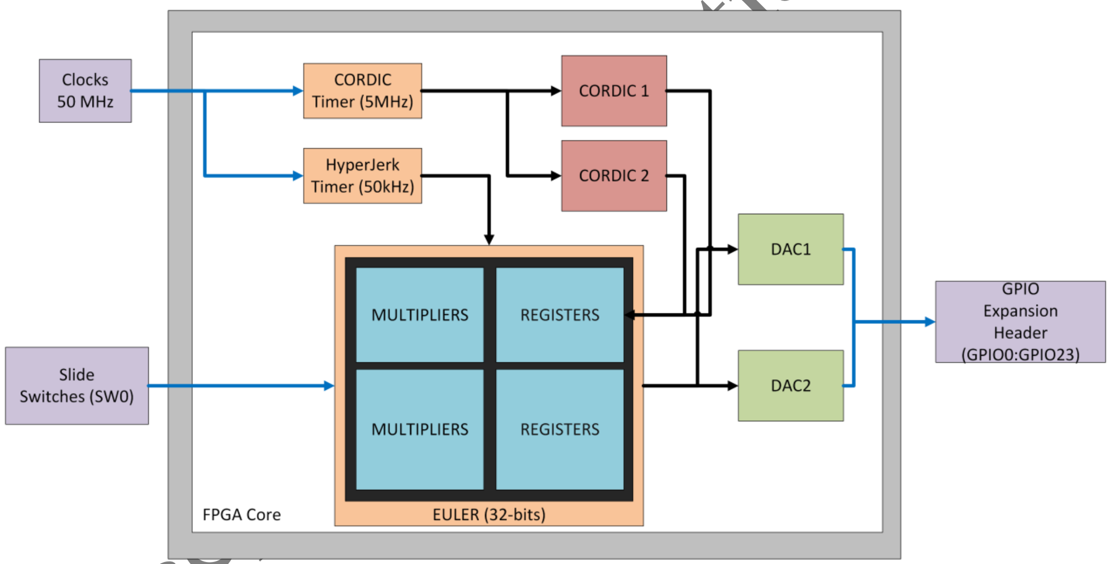

Figure 7: Block diagram for implementing the proposed Hyperjerk system on an FPGA board.

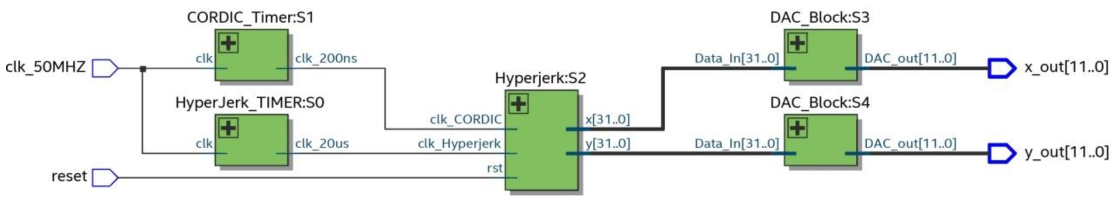

Figure 8: RTL schematic for the realization of the proposed Hyperjerk system.

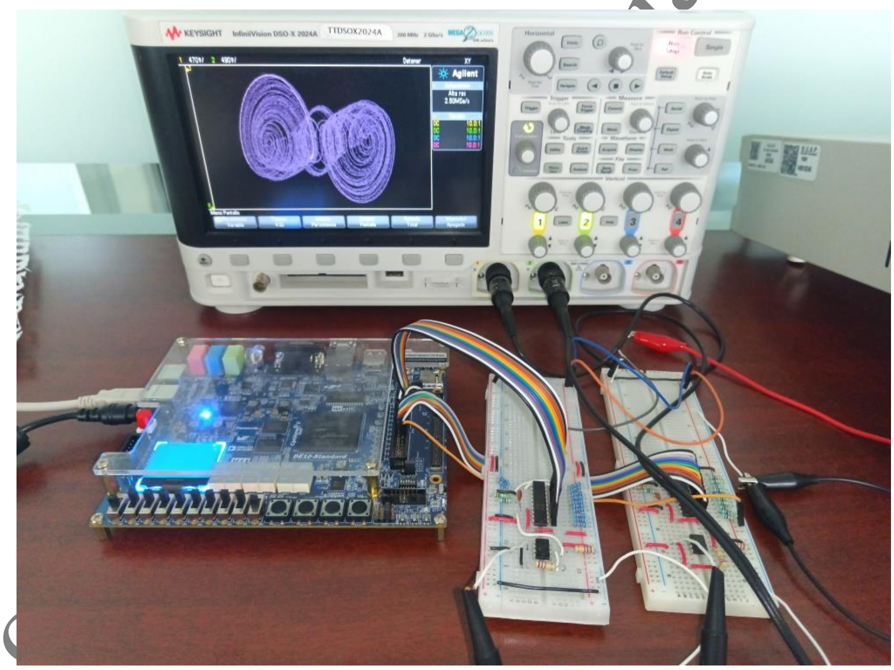

Figure 9: Hardware realization of the proposed system in FPGA technology.

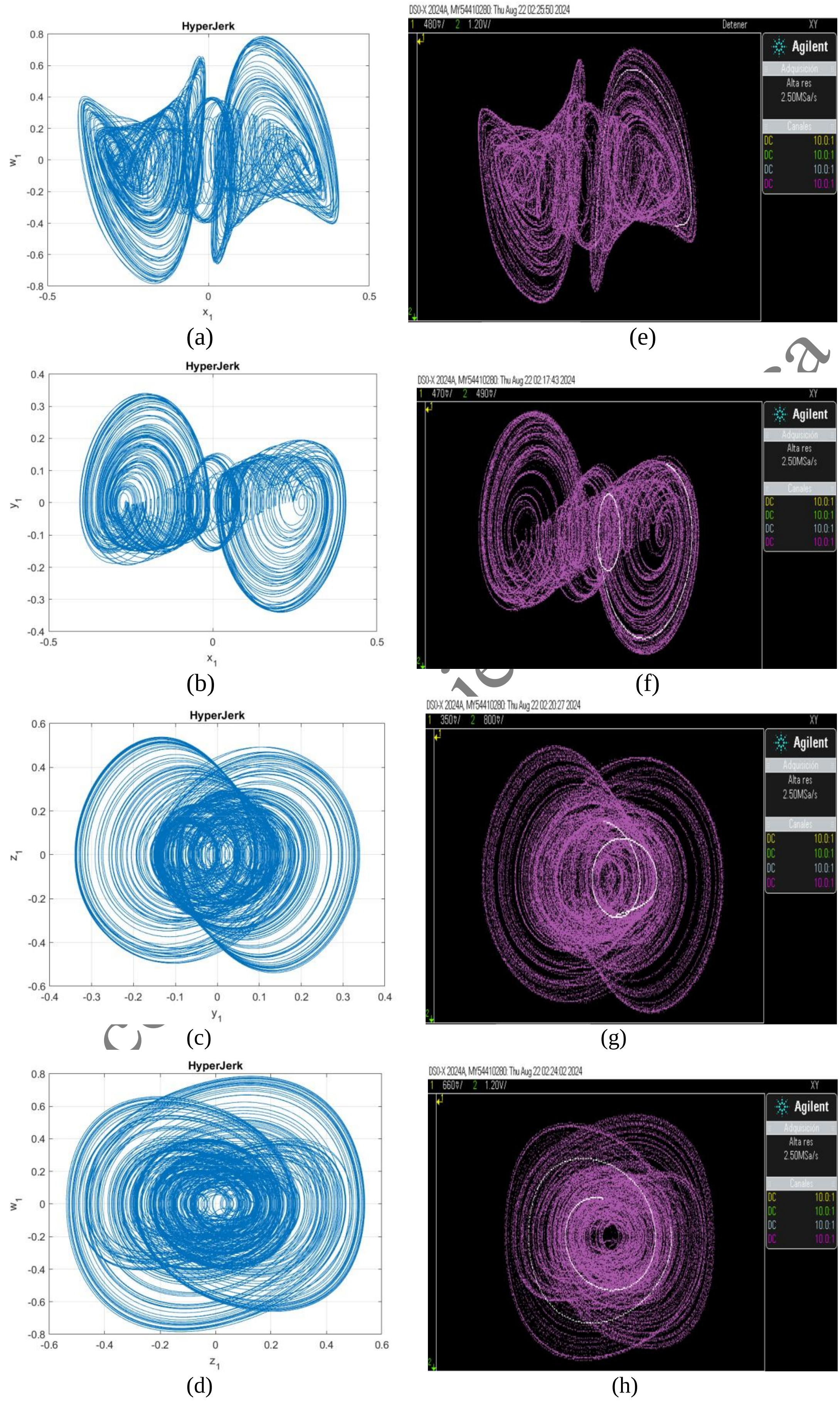

Figure 10: Comparison of the FPGA implementation of the new chaotic HyperJerk system versus Matlab numerical simulations

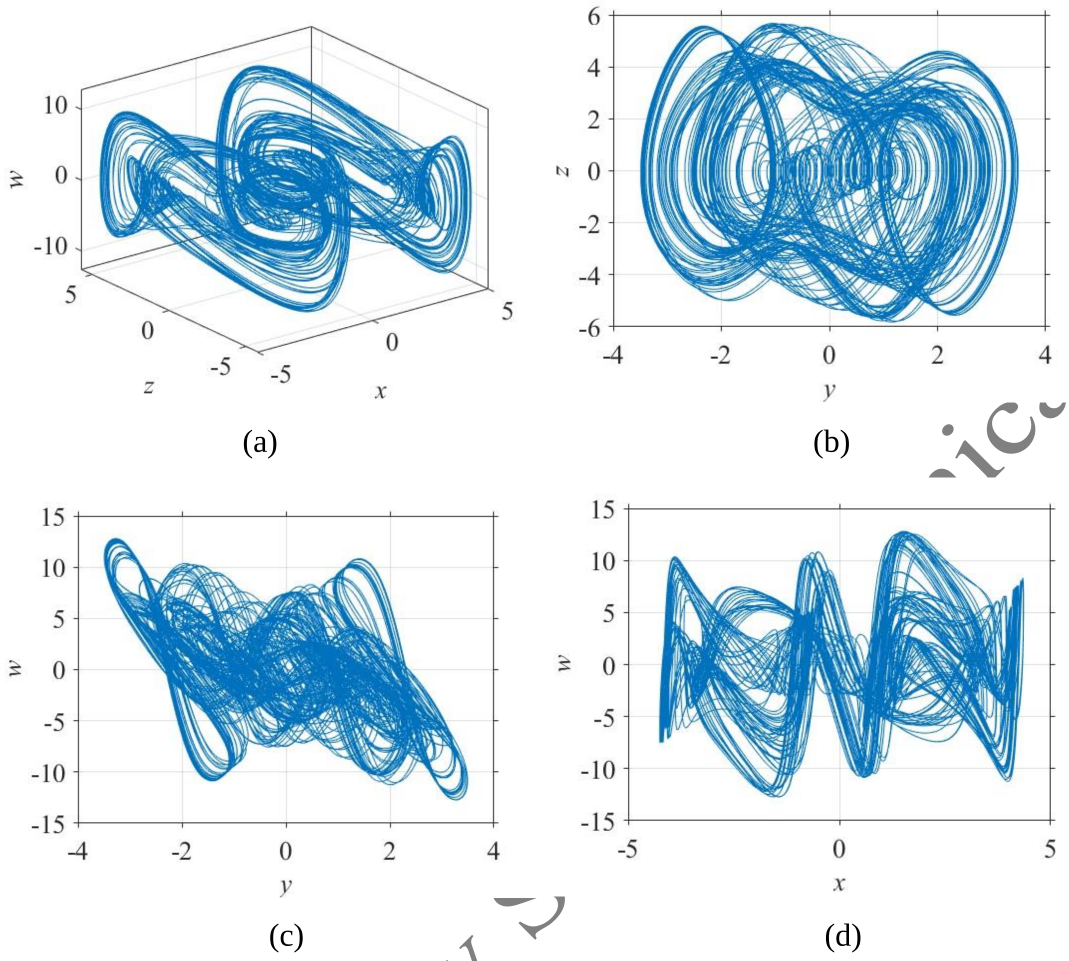

Figure 11: The phase projections of FOHJ system (10) in various planes

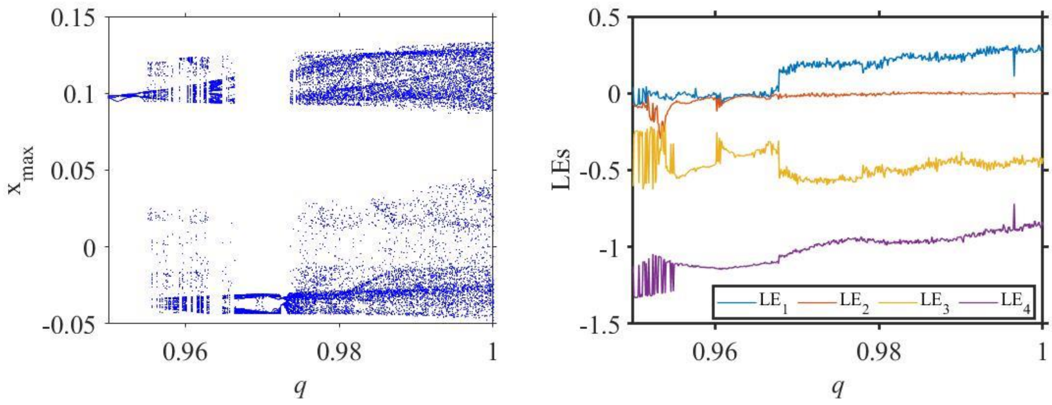

Figure 12: (a) Bifurcation (b) LE plot of FOHJ system (10) for fractional order *q*

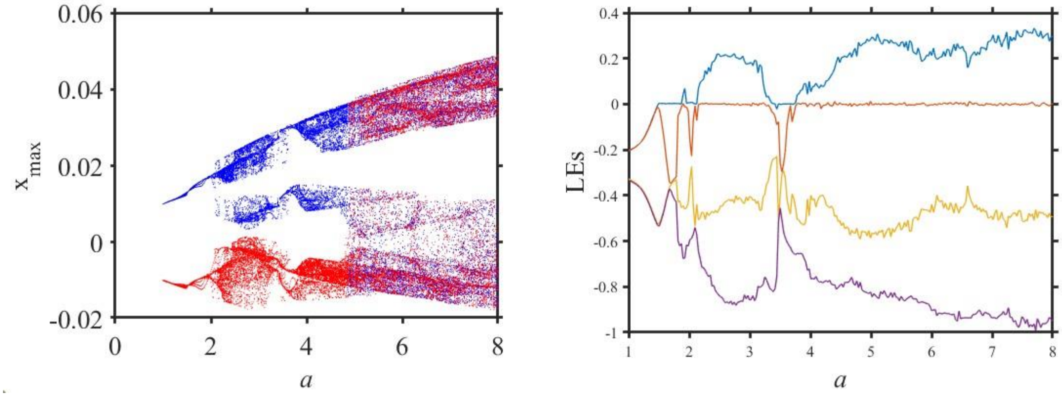

(a) (b)

Figure 13: (a) Bifurcation plot (b) LEs plot of FOHJ system (10) for the parameter *a*

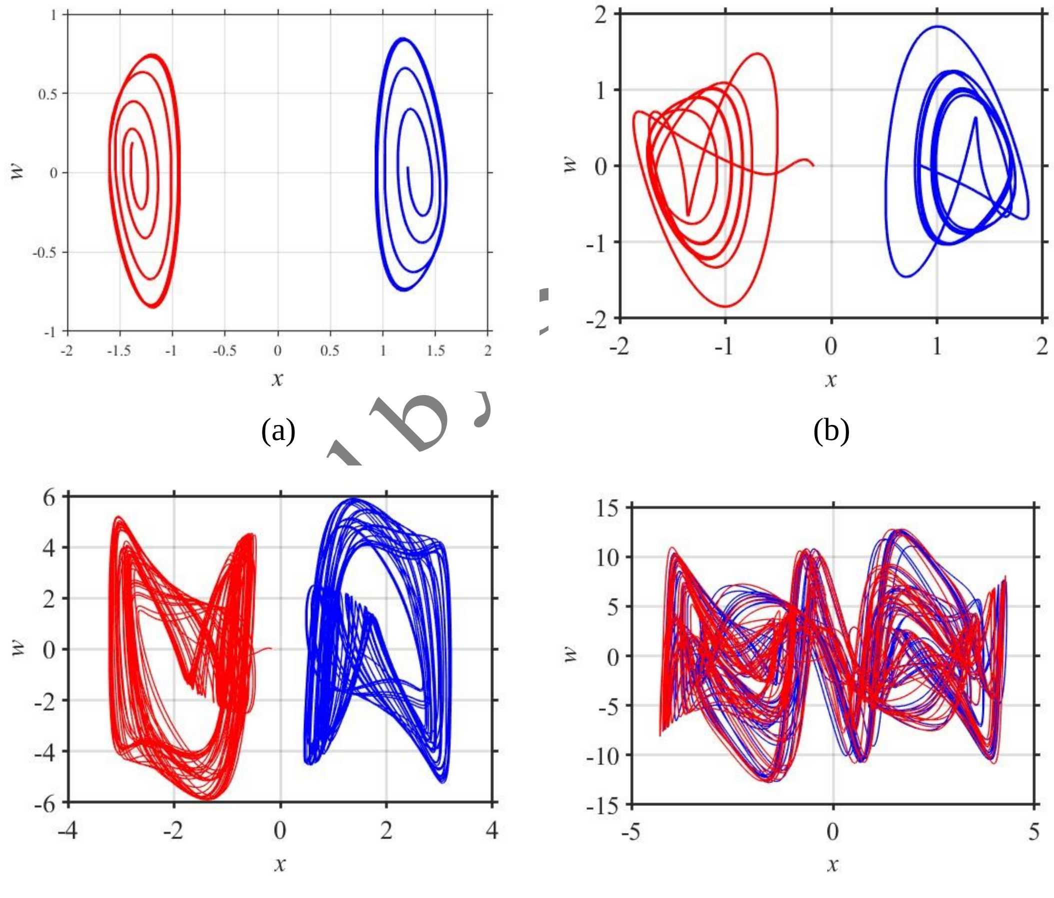

Figure 14: The coexisting attractors of FOHJ system (10) when (a) a = 1.8, (b) a = 2, (c) a = 4 and (d) a = 6 respectively.

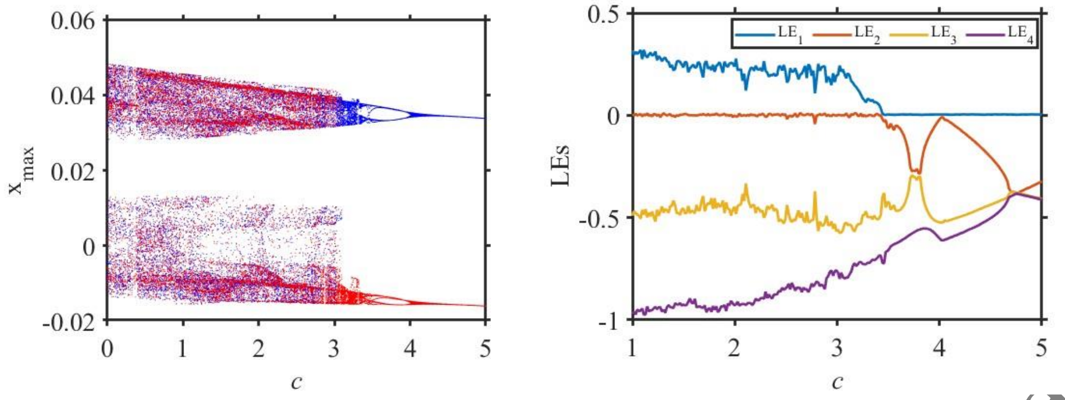

Figure 15: (a) Bifurcation behavior (b) LE plot of FOCHJ system (10) for *c*

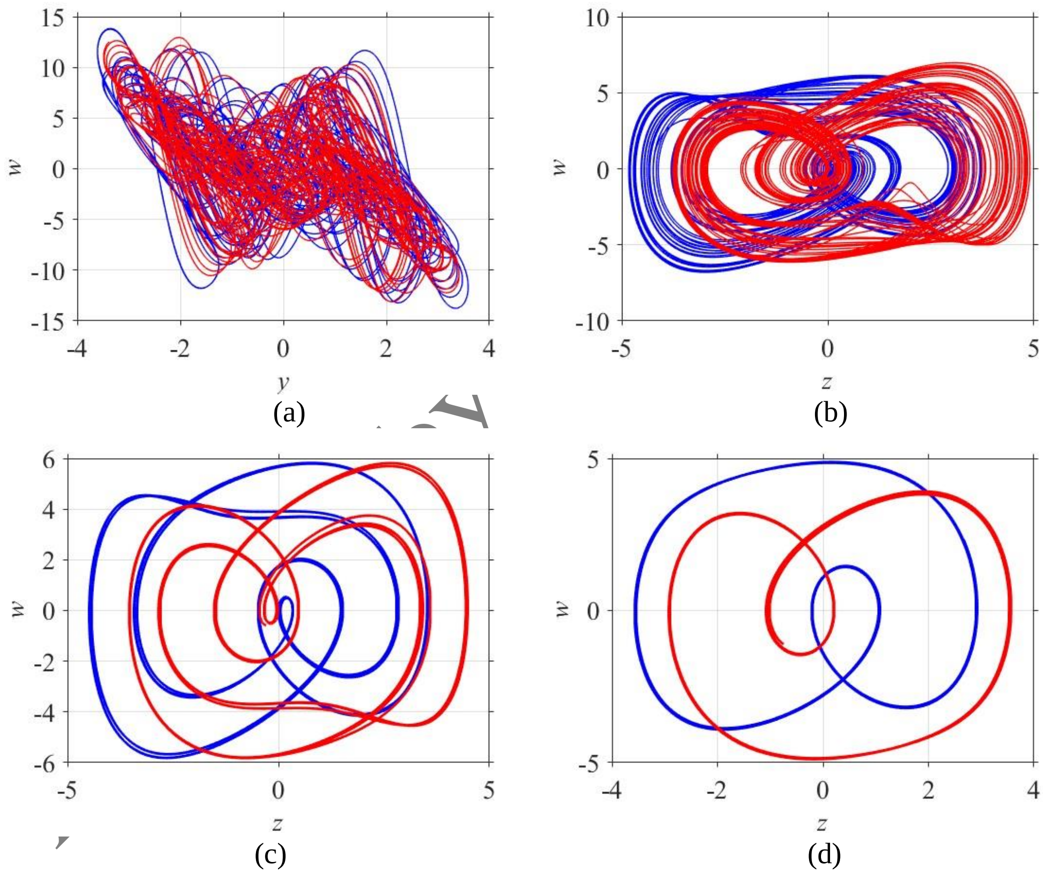

Figure 16: The coexisting attractors of FOHJ system (10) when (a) c = 1, (b) c = 3.2, (c) c =3.6 and (d) c =4.5.

Table 1: Resources utilization by Entity and Total of the FPGA implementation of hyperjerk system.

Entity	**Combinational ALUTs**	**Dedicated Logic Registers**	**DSP Blocks**	**Pins**
Hyperjerk	300	128	0	0
Euler	1928	481	72	0
HyperJerk_Timer	43	33	0	0
CORDIC_Timer	43	33	0	0
DACs	88(44)	0	6(3)	0
Total	2154	675	78	26

Table 2: Power consumption and operating frequency comparison of the proposed Hyperjerk system.

		This work	Gugapriya et al [39]	Karakaya et al [40]	Mohammad et al [41]
Power	Dynamic	22.03 mW	139 mW	N/A	N/A
	Static	412.81 mW	159 mW	N/A	N/A
	I/O	9,83 mW	91 mW	N/A	N/A
	Total	444.67mW	298 mW	N/A	N/A
Max. Frequency		90.69MHz	Not reported	59.492 MHz	73.83 MHz
Bit Throughput		5.804 Gbps	N/A	3.807 Gbps	1.772 Gbps
Reported behavior		Hyperjerk	Double scroll	Double scroll	Hyperchaos